Astron. Astrophys. 362, 635–645 (2000)

ASTRONOMY AND ASTROPHYSICS

Submillimeter maps of small young clusters in three large globules

T.L. Huard[1], **D.A. Weintraub**[1], **and G. Sandell**[2]

[1] Department of Physics and Astronomy, Vanderbilt University, P.O. Box 1807 Station B, Nashville, TN 37235, USA (tracy.huard,david.weintraub@vanderbilt.edu)

[2] National Radio Astronomy Observatory*, P.O. Box 2, Green Bank, WV 24944, USA (gsandell@nrao.edu)

Received 24 November 1999 / Accepted 4 May 2000

Abstract. We present submillimeter maps of regions within three large globules, CB 3, CB 34, and L 810. Our maps are centered on three IRAS sources, each of which is associated with a small cluster of near-infrared young stellar objects (YSOs) as seen from deep optical and/or near-infrared observations. We have detected submillimeter sources associated with the YSO clusters. The submillimeter emission appears to be primarily from small clusters of protostars rather than from the sources previously detected in the near-infrared. This result suggests that these large globules are currently adding protostars to these clusters. Thus, star formation within each of these large globules appears to be a continuous process rather than a single, isolated event.

Key words: stars: formation – stars: pre-main sequence – ISM: clouds – ISM: dust, extinction – ISM: individual objects: CB34 L810

1. Introduction

Most of the molecular clouds of small angular extent (Clemens & Barvainis 1988; Bourke et al. 1995) are physically small and nearby. Such clouds, known as Bok globules, are often sites of star formation typically containing only a few forming stars (Huard et al. 1999; Yun & Clemens 1990, 1994b). However, some clouds of small angular extent are actually physically large and distant (beyond 1 kpc). Such clouds are referred to as "large globules." Because large globules have small apparent diameters, young stellar objects (YSOs) observed in the vicinity of large globules are likely associated with the globules. Since large globules are much more massive than Bok globules, star formation within such globules tends to produce small stellar clusters rather than aggregates of only a few stars.

Surveys of the YSO populations of nearby clouds demonstrate that stellar cluster formation in these clouds is a continuous process, rather than a relatively instantaneous event (e.g., Sandell & Knee 2000, Motte et al. 1998, Testi & Sargent 1998). Since the sizes and masses of large globules are comparable to those of nearby, star-forming molecular clouds, we might expect the YSO populations of large globules to be similar to those of the nearby clouds. Because large globules have small angular extents, YSO surveys of large globules can be done efficiently without mapping a large region of the sky.

YSOs of different evolutionary stages are detectable in different regions of the spectrum. Very young protostars, known as Class 0 sources, are surrounded by large amounts of cold dust and are sources of outflows. Thus, protostars are detected by the submillimeter continuum emission from the surrounding dust or by molecular line observations identifying outflow activity. Since the optical depths at near-infrared wavelengths are very large toward protostars, they are never detected in near-infrared observations. More evolved YSOs, referred to as Class I and Class II sources, are surrounded by less dust and thus are faint in the submillimeter. However, because the central stars of the Class I or Class II sources are less obscured, these sources are observed as heavily reddened near-infrared souces.

Submillimeter mapping offers the best way to identify the young, protostellar population within a star-forming region. As an initial probe of current star formation activity within star-forming large globules, we have mapped cold IRAS sources associated with the large globules CB 3, CB 34, and L 810 in the submillimeter continuum. The colors of the associated IRAS sources suggest that these large globules currently are forming stars. Furthermore, the IRAS sources are known to be in the vicinity of clusters of YSOs, seen in near-infrared surveys, which have formed within these globules.

2. Observations

Using the submillimeter common user bolometer array SCUBA (Gear & Cunningham 1995) on the James Clerk Maxwell Telescope (JCMT)[1], we obtained 450 μm and 850 μm maps of IRAS 00259+5625 (in CB 3) and IRAS 19433+2743 (in L 810) on 1997 December 18, and IRAS 05440+2059 (in CB 34) on

Send offprint requests to: T.L. Huard

* The National Radio Astronomy Observatory is a facility of the National Science Foundation operated under cooperative agreement by Associated Universities, Inc.

[1] The JCMT is operated by the Joint Astronomy Centre, on behalf of the UK Particle Physics and Astronomy Research Council, the Netherlands Organization for Scientific Research, and the Canadian National Research Council.

1998 February 15. These IRAS sources are among the brightest 100 μm sources associated with globules listed in the Clemens & Barvainis (1988) catalog. Our maps, covering at least $1\farcm5 \times 1\farcm5$ regions approximately centered on each IRAS source, represent 5–10% of the optical core regions within CB 3 and L 810 and more than half of the optical core of CB 34. Most of the members of the known near-infrared clusters associated with these large globules lie within the regions covered by our submillimeter maps. We reduced the submillimeter maps using the methods described in the SCUBA mapping cookbook (Sandell 1997). The final maps were calibrated in units of Jy beam^{-1} from maps of Uranus and the secondary calibrators RAFGL 618 and RAFGL 2688 (Sandell 1994)[2]. We estimate that the 450 μm and 850 μm flux calibration errors are less than 30% and 15%, respectively. The submillimeter opacities at 450 μm and 850 μm were estimated from the sky dip meter located at Caltech Submillimeter Observatory, which provides opacity information at 1300 μm every 10 minutes. Our data were collected on nights with good atmospheric conditions when the 850 μm opacity was as low as 0.16, providing stringent upper limits for undetected sources at both 450 μm and 850 μm. In order to derive accurate positions, a nearby source of known position was observed before and after mapping each region. Consequently, the pointing uncertainties are less than $\sim$2 arcseconds in all maps.

SCUBA has 37 bolometers in the long (850 μm) wavelength array and 91 bolometers in the short (450 μm) wavelength array; the bolometers of each array are separated by approximately two beam widths in a hexagonal pattern. The half power beam width (HPBW) of SCUBA is $\sim 8\farcs0$ at 450 μm and $\sim 15''$ at 850 μm. Both arrays can be used simultaneously. We used the 850 μm + 450 μm filter combination in jiggle-map mode as described in Huard et al. (1999).

3. Results

We present the SCUBA maps in Figs. 1–3. The coordinates for all the submillimeter sources detected in this survey are listed in Table 1. Taking into consideration the pointing accuracy of our maps ($\leq 2''$) and the uncertainty associated with determining the position of a submillimeter source ($\sim 1''$), we estimate that the positions listed in Table 1 are accurate to within $\sim 3''$. The positions of all known optical and near-infrared sources located within the fields are overlayed on each map for comparison with the positions of the submillimeter sources.

The properties of the submillimeter sources derived from our SCUBA maps are listed in Table 2. The peak flux densities, deconvolved full-width-at-half-maxima (FWHM) sizes, total fluxes, and total (gas + dust) masses were determined as described in Huard et al. (1999). The total mass was derived from:

[2] See the notes concerning secondary calibrators posted on the Joint Astronomy Centre Web site at the following address: http://www.jach.hawaii.edu/JCMT/scuba/astronomy /calibration/calibrators.html

Table 1. Positions of Compact Submillimeter Sources

Submillimeter Source	α (2000.0)	δ (2000.0)
CB 3: SMM1	$00^h\ 28^m\ 44.2^s$	$+56^\circ\ 42'\ 01''$
CB 34: SMM1	$05^h\ 47^m\ 01.9^s$	$+21^\circ\ 00'\ 06''$
CB 34: SMM2	$05^h\ 47^m\ 00.0^s$	$+21^\circ\ 00'\ 30''$
CB 34: SMM3	$05^h\ 47^m\ 05.3^s$	$+21^\circ\ 00'\ 42''$
CB 34: SMM4	$05^h\ 47^m\ 05.2^s$	$+21^\circ\ 00'\ 25''$
CB 34: SMM5[a]	$05^h\ 47^m\ 07.8^s$	$+21^\circ\ 00'\ 04''$
L 810: SMM1	$19^h\ 45^m\ 23.9^s$	$+27^\circ\ 51'\ 02''$
L 810: SMM2	$19^h\ 45^m\ 21.3^s$	$+27^\circ\ 50'\ 40''$

[a] Because this submillimeter source was not fully mapped in our observations, the position is uncertain.

$$M_{tot} = \frac{S_\nu D^2}{\kappa_\nu B_\nu(T_{\rm dust})} \left(\frac{M_{\rm gas}}{M_{\rm dust}}\right),$$

where S_ν is the observed total flux at frequency ν, D is the distance to the source, $B_\nu(T_{\rm dust})$ is the Planck blackbody function at the dust temperature $T_{\rm dust}$, and κ_ν is the dust opacity. The dust opacity is given by $\kappa_\nu = \kappa_0(\nu/\ 1.2\times10^{12}\ {\rm Hz})^\beta\ {\rm cm^2\ g^{-1}}$ where $\kappa_0 = 0.1\ {\rm cm^2\ g^{-1}}$ (Hildebrand 1983) and β is the dust emissivity index. Except in the case of CB 34: SMM4 (where we use the 450 μm flux), we use the 850 μm fluxes for the purpose of estimating the masses of the sources. We adopt β = 1.3, comparable to previously published emissivities for protostars (Huard et al. 1999; Visser et al. 1998; Chandler & Sargent 1993; Wright et al. 1992), a gas-to-dust mass ratio of 100, and $T_{\rm dust}$ = 25 K. For comparison with our estimates of the total masses, we list virial masses, assuming a mass density profile inversely proportional to the distance from the center of the source, calculated from:

$$M_{\rm virial} = 190 R(\Delta v)^2$$

where R is the radius in parsecs and Δv is the linewidth in km s^{-1} (MacLaren et al. 1988). We set R = FWHM/2, where we use the FWHM determined from our 450 μm observations, except in the case of CB 34: SMM2 where we use the FWHM determined from the 850 μm observations. The linewidths were taken from the results of previous studies. Finally, we list the bolometric luminosities. These luminosities were determined by integrating the entire spectral energy distributions over all wavelengths, extrapolated from the submillimeter fluxes assuming $T_{\rm dust}$ = 25 K. Thus, the bolometric luminosities listed in Table 2 represent the total luminosities from the cold dust within these environments, including the mid-infrared, far-infrared, and submillimeter regions of the spectrum where there exists significant emission from cold dust. The IRAS fluxes were not specifically used in these calculations because they include flux from the larger portions of the cloud as well as the submillimeter sources, rather than from only the submillimeter sources themselves.

Many of the sources observed in our maps are resolved at both 450 μm and 850 μm (Table 2). To illustrate how strongly resolved these sources are, we present azimuthally averaged, radial flux density profiles for CB: 3 SMM1 and RAFGL 618

Table 2. Properties of Submillimeter Sources in Large Globules

Submillimeter	Peak Flux Density[a] (Jy/beam)		Deconvolved FWHM[b] (10^3AU)		Total Flux (Jy)		M^c_{tot}	M_{virial}	L_{bol}
Source	450 μm	850 μm	450 μm	850 μm	450 μm	850 μm	($M_\odot$)	($M_\odot$)	($L_\odot$)
CB 3: SMM1	7.9	1.5	17.5×12.5	$30 \times < 12.5$	13	2.0	40	20[i]	400
CB 34: SMM1	0.88	0.29	18×9	24×18	2.1	0.53	4	9[j]	40
CB 34: SMM2	0.74[d]	0.20	–[e]	52.5×40.5	–	1.0	8	10[k]	70
CB 34: SMM3	1.2	0.49	40.5×28.5	36×24	12	1.4	10	10[k]	100
CB 34: SMM4	0.66	–[f]	15×12	–[f]	1.6	–	2	4[k]	20
CB 34: SMM5	–[g]	0.18[d]	–	–[e,h]	–	0.18[d,h]	1	2[k]	10
L 810: SMM1	1.6	0.32	34×16	50×22	5.7	0.77	10	10[l]	90
L 810: SMM2	0.96	0.20	$< 10 \times < 10$	$< 10 \times < 10$	0.96	0.20	3	5[l]	20

[a] Unless otherwise noted, background dust emission seen in the direction of the globule has been subtracted before determining the peak flux density.
[b] Distances to CB 3, CB 34, and L 810 are assumed to be 2.5, 1.5, and 2.0 kpc, respectively.
[c] Total (gas + dust) mass of the submillimeter source, excluding the mass associated with the surrounding cloud. (Launhardt & Henning 1997).
[d] Because background emission could not be determined reliably, emission from both the submillimeter source and globule dust is included.
[e] Unable to fit source to a two-dimensional Gaussian profile.
[f] Source is blended with a brighter submillimeter source at this wavelength.
[g] Our 450 μm map does not cover this region of the globule core.
[h] Source is assumed to be unresolved.
[i] Virial mass is based on Δv=1.6 km s^{-1} observed in C^{18}O by Wang et al. (1995).
[j] Virial mass is based on Δv=1.22 km s^{-1} observed in NH_3 by Codella & Scappini (1998).
[k] Virial mass is based on an assumed Δv=0.8 km s^{-1}, the median NH_3 linewidth for protostellar cores associated with IRAS sources (Jijina et al. 1999).
[l] Virial mass is based on Δv=1.0 km s^{-1} observed in NH_3 by Neckel et al. (1985).

Table 3. Globule Dust Emission

Large	Total Integrated Flux (Jy)		Mass[a]
Globule	450 μm	850 μm	($M_\odot$)
CB 3	$\lesssim 8$	1.5	110
CB 34	8.2	2.8	80
L 810	22	2.9	120

[a] Total (gas + dust) mass associated with the surrounding cloud in the field, excluding the mass associated with embedded submillimeter sources.

in Fig. 4. CB 3: SMM1 is the smallest resolved source that we observed. In comparison, RAFGL 618 appears as an unresolved or marginally resolved source (refer to footnote 2 on the previous page), representing the 450 μm and 850 μm beam profiles. It is immediately evident from Fig. 4 that all of our sources, for which we present FWHM in Table 2, are extended at both 450 μm and 850 μm.

The total fluxes at 450 μm and 850 μm from the dust associated with the dark clouds surrounding the sources are given in Table 3. For each field, the globule flux, which does not include the flux from the compact sources, was determined by integrating over the entire region showing extended emission. This flux was normalized by the beam integral, assuming the beam profile is Gaussian, and the contribution from the extended error lobe was removed. The error lobe contribution is small at 850 μm, but at 450 μm it is of the same order as the total integrated emission. The total flux from the submillimeter sources in the field were then subtracted, giving the total flux contribution due to the surrounding dark cloud. To estimate the total mass of the gas and dust in the surrounding cloud based on the total 850 μm flux, we adopt a gas-to-dust mass ratio of 100, $T_{\rm dust}$ = 20 K, and $\beta_{\rm cloud}$ = 2, consistent with emissivities for dust in the interstellar medium and the dark clouds surrounding protostars (Huard et al. 1999; Visser et al. 1998). Because our observations are sensitive to only the denser regions of dust emission, these mass estimates (Table 3) should be considered lower limits.

IRAS 00259+5625 in CB 3

Fig. 1 shows our submillimeter maps of the field toward IRAS 00259+5625, the only IRAS source within CB 3 (also known as LBN 594). Our 850 μm map shows an extended dust cloud elongated in the north-south direction with a second cloud component to the northwest. In the dense central cloud core, we find a "compact" submillimeter source, CB 3: SMM1, about 15″ west and 6″ south of the IRAS source, in reasonable agreement with the position of the 1.3 mm continuum source observed by Launhardt & Henning (1997).

The overall morphology of the dust emission is similar to the C^{18}O map of Wang et al. (1995), although the C^{18}O emission is more extended than the dust emission. The similarity is much better when we compare our SCUBA maps to maps of high density tracers like CS

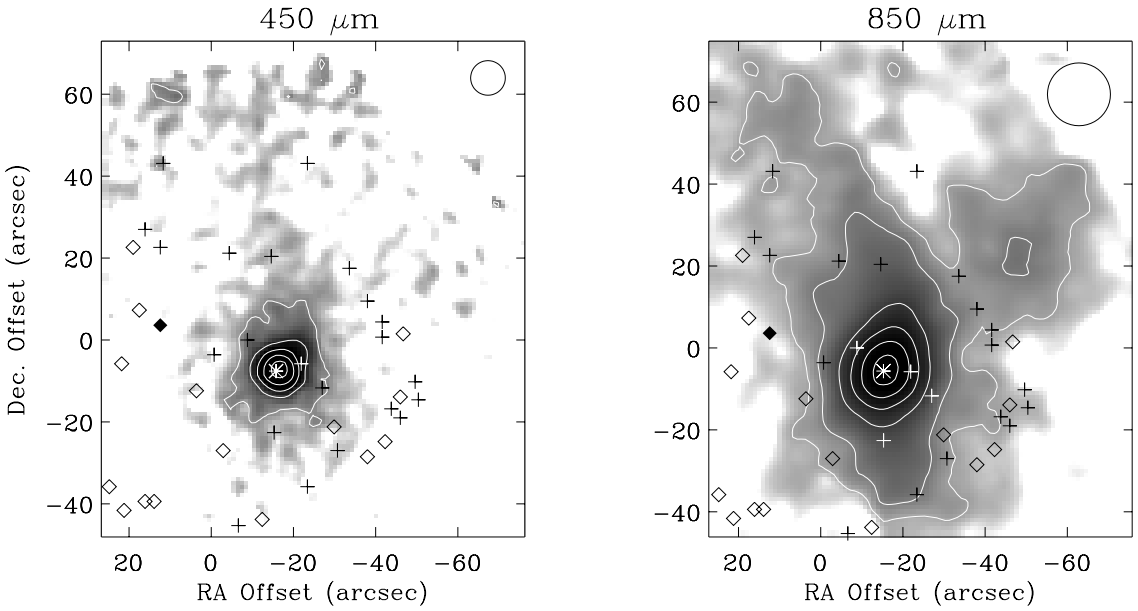

Fig. 1. 450 μm and 850 μm jiggle maps of the IRAS 00259+5625 field associated with CB 3. The origin is located at the nominal IRAS source position. The position of CB 3: SMM1 is identified by an asterisk at ($-15''$, $-6''$). The contours at 450 μm are drawn at 10, 30, 50, 70, and 90% of the CB 3: SMM1 peak (8.0 Jy beam^{-1}), while the contours at 850 μm are drawn at 5, 10, 30, 50, 70, and 90% of the CB 3: SMM1 peak (1.7 Jy beam^{-1}). The 3-σ noise levels of the maps are 0.79 and 0.067 Jy beam^{-1} at 450 μm and 850 μm, respectively. The very red K sources located within the field are identified in our maps by plus signs, while the other K sources within the field are identified by open diamonds (Launhardt et al. 1998b). The near-infrared source CB3YC1-I, suggested to be an embedded PMS star by Yun & Clemens (1994b), is identified by a filled diamond.

(Codella & Bachiller 1999; Launhardt et al. 1998a) or SO and $H^{13}CO^+$ (Codella & Bachiller 1999). The maps tracing the high density gas show a closer positional agreement between the high density gas and the cloud core. These gas tracers also show an extension to the northwest, in rough agreement with the position of the second cloud core observed in our 850 μm SCUBA map. The extended nature of the northwestern core, combined with the lack of 450 μm emission, suggests that this core is a cold prestellar core without any embedded sources. The closest near-infrared source to CB 3: SMM1 is offset by $\sim 7''$ (see Fig. 1), well beyond the positional uncertainties associated with the near-infrared and submillimeter sources.

We derive a mass of 40 $M_\odot$ for CB 3: SMM1 (not including the mass of the surrounding gas and dust associated with the cloud; Table 2), a factor of two lower than the mass of 80 $M_\odot$ derived by Launhardt et al. (1997) and 72 $M_\odot$ derived by Launhardt & Henning (1997). Both of the larger estimates include the mass of the surrounding cloud within the beams as well as the mass of the submillimeter source.

We estimate that the cloud has a total mass of at least $\sim$150 $M_\odot$ (Tables 2 & 3) if we include the mass of CB 3: SMM1. This estimate is consistent with previous estimates based on $C^{18}O$ and H_2CO (Wang et al. 1995) as well as CS molecular line observations (Launhardt et al. 1998a). The $C^{18}O$ map of this region reveals a high density core region of 67–230 $M_\odot$ (centered $\sim 16''$ northwest of CB 3: SMM1 and extending across a region $95'' \times 40''$ in size), approximately coinciding with CB 3: SMM1 and the surrounding cloud core. Launhardt et al. (1998a) derive a mass of 99 $M_\odot$ associated with the $41'' \times 24''$ CS core (a smaller region than that showing submillimeter emission in our maps) centered only $\sim 7''$ northwest of CB 3: SMM1. However, Codella & Bachiller (1999), assuming a homogenous spherical cloud of $40''$, derive a mass as large as $\sim$550 $M_\odot$, which is far more than that indicated by our submillimeter dust observations.

The deep near-infrared maps of the region of CB 3 (Launhardt et al. 1998b) included within our submillimeter maps show many near-infrared sources, 22 of which are very red, indicative of embedded PMS stars and none of which are coincident with CB 3: SMM1. In addition to having several dozen PMS stars, CB 3 is known to be associated with at least one molecular outflow (Codella & Bachiller 1999; Yun & Clemens 1994a; Yun & Clemens 1992), the center of which is coincident (to within positional uncertainties) with the position of CB 3: SMM1. The presence of a submillimeter source with an outflow and no near-infrared counterpart indicates that CB 3: SMM1 is most likely one or more Class 0 sources. The mass (40 $M_\odot$) of CB 3: SMM1 is far too large for a relatively low luminosity Class 0 source to be a single protostar, and we suggest CB 3: SMM1 harbors more than one protostar. The 450 μm emission of CB 3: SMM1 (see the 30% contour) appears to have an extension toward the northwest, which may indicate a second embedded source. Furthermore, inspection of the CO J = 2−1 maps of Codella & Bachiller (1999) suggests there may be a second molecular outflow. Specifically, a secondary redshifted component toward the northwest and a corresponding secondary blueshifted component toward the

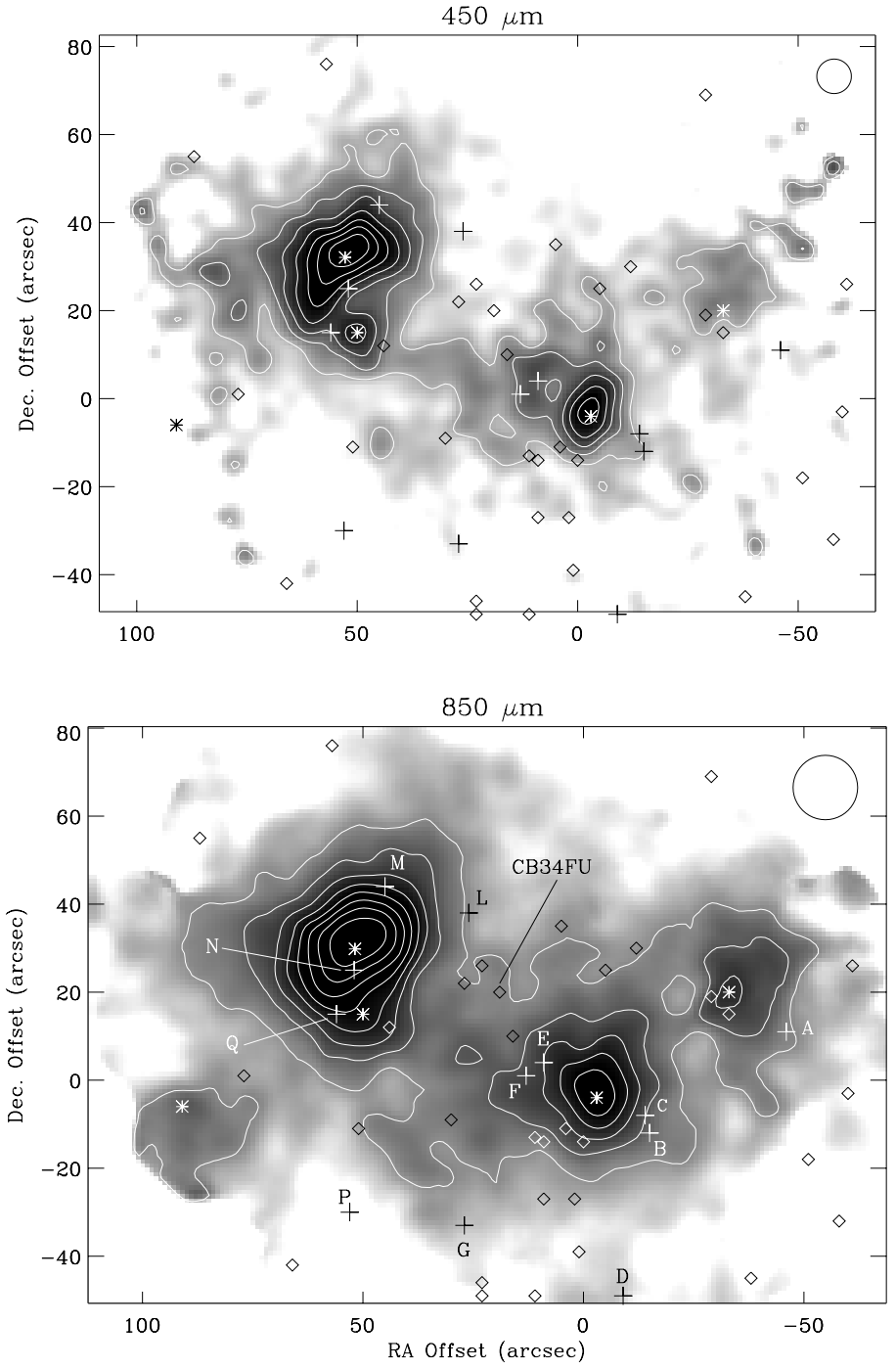

Fig. 2. 450 μm and 850 μm jiggle maps of the IRAS 05440+2059 field associated with CB 34. The origin is located at the nominal IRAS source position. The positions of CB 34: SMM1, CB 34: SMM2, CB 34: SMM3, CB 34: SMM4, and CB 34: SMM5 are identified by asterisks at ($-3''$, $-4''$), ($-33''$, $20''$), ($51''$, $32''$), ($50''$, $15''$), and ($91''$, $-6''$), respectively. The contours at 450 μm are drawn at 30, 40, 50, 60, 70, 80, and 90% of the CB 34: SMM3 peak (1.7 Jy beam^{-1}), while the contours at 850 μm are drawn at 20, 30, 40, 50, 60, 70, 80, and 90% of the CB 34: SMM3 peak (0.61 Jy beam^{-1}). The 3-σ noise levels of the maps are 0.25 and 0.084 Jy beam^{-1} at 450 μm and 850 μm, respectively. The near-infrared sources located within the field are indicated by either plus signs or open diamonds, where the plus signs are those sources exhibiting near-infrared excesses and labeled using the notation of Alves & Yun (1995).

southwest are evident in their maps. These secondary outflow components do not appear to be part of the large north-south outflow.

Yun & Clemens (1995) classified CB3YC1-I, a very red, near-infrared source lying $\sim 10''$ north and $\sim 27''$ east of CB 3: SMM1, as Class II-D because the composite spectrum formed from the near-infrared fluxes from CB3YC1-I and the IRAS fluxes of IRAS 00259+5625 is double-peaked. Given that CB 3: SMM1 and many near-infrared sources lie very close to the nominal IRAS source position, the IRAS flux densities are certainly affected by many sources. Assuming a temperature of 25 K and β=1.3, we find the 60 μm and 100 μm IRAS flux densities appear to be due entirely to CB 3: SMM1, with no contribution from CB3YC1-I. Thus, CB3YC1-I appears to be a Class II rather than a Class II-D source. This situation may be the case for other Class II-D sources as well. The near-infrared spectrum of CB3YC1-I is consistent with that of a 2300 K blackbody.

IRAS 05440+2059 in CB 34

We present in Fig. 2 our submillimeter maps of the region of globule CB 34 toward IRAS 05440+2059, the only IRAS source

within this large globule. In an attempt to cover most of the submillimeter emission seen toward this globule, we made a small mosaic. Our maps show that CB 34 contains dust emission stretching across a region about 1 pc wide. Since the dust emission is very extended, it is likely that we have chopped onto emission outside our field of view. Therefore, our estimates for the total flux from this region should be considered lower limits. We identify five submillimeter sources within the field.

The nominal position of IRAS 05440+2059 is very nearly coincident with the position of CB 34: SMM1, suggesting that CB 34: SMM1 is the submillimeter counterpart to IRAS 05440+2059. No near-infrared sources are found within $\sim 10''$ of CB 34: SMM1. The bright 450 μm emission region associated with CB 34: SMM1 is very elongated with a position angle of $\sim 160°$, approximately perpendicular to the outflow axis. The outflow map (Yun & Clemens 1992; Yun & Clemens 1994a) shows a second blue-shifted outflow lobe, indicating there may be two outflows in the region surrounding CB 34: SMM1. Given the large size ($\sim$10,000 AU) and elongation of CB 34: SMM1, as well as evidence suggesting two outflows, we suggest that CB 34: SMM1 may represent blended emission from two Class 0 protostars.

CB 34: SMM2, found to the northwest of CB 34: SMM1, is fainter and more extended than CB 34: SMM1 at both 450 μm and 850 μm. The position of CB 34: SMM2 is $\sim 4''$ from any near-infrared source and $\sim 16''$ from source A, the closest source exhibiting near-infrared excess. We suggest that CB 34: SMM2 is another protostellar source.

The shape of the brightest submillimeter source in our maps, CB 34: SMM3, suggests that the source represents blended emission from several submillimeter sources. In fact, the submillimeter source we identify as CB 34: SMM4 is blended with CB 34: SMM3 at 850 μm, appearing as a distortion of the lower level contours surrounding CB 34: SMM3. At 450 μm, CB 34: SMM4 is clearly resolved from CB 34: SMM3. The closest near-infrared sources to CB 34: SMM3 and CB 34: SMM4 are sources N and Q, lying $\sim 7''$ from these submillimeter sources, respectively. Both of these near-infrared sources have been identified as YSOs based on their near-infrared colors (Alves & Yun 1995). CB 34: SMM3 and CB 34: SMM4 likely represent a more recent generation of star formation within this region of the CB 34 core.

We identify the faintest submillimeter source, located in the southeastern portion of the field at 850 μm, as CB 34: SMM5. This region of CB 34 was not covered by the more limited field of view of the 450 μm array. No near-infrared sources are seen near the position of CB 34: SMM5 in the previously published, near-infrared map (Alves & Yun 1995). We suggest that CB 34: SMM5 may be another site of current star formation within CB 34.

We derive a mass of 4 $M_\odot$ for CB 34: SMM1 based on the 850 μm flux (not including the mass of the surrounding gas associated with the cloud; Table 2). Our result is consistent with the mass estimates of 5.9 $M_\odot$ derived by Launhardt & Henning (1997) and 11 $M_\odot$ Launhardt et al. (1997). Both of the larger estimates include the mass of the surrounding cloud within the beams as well as the mass of the submillimeter source. We estimate that the combined mass of all five submillimeter sources and the mass of the surrounding cloud is $\sim$110 $M_\odot$ (Tables 2 and 3). Keeping in mind that our observations are only sensitive to the densest regions of the globule and therefore represent only a lower limit on the globule mass, our derived globule mass is consistent with the previous estimate of 170 $M_\odot$ based on CS (Launhardt et al. 1998a).

Despite evidence that almost all FU Orionis stars are bright enough (Sandell & Weintraub in preparation; Weintraub & Sandell 1991) to be detectable in the submillimeter even at distances of 1.5 kpc, we failed to detect a submillimeter counterpart to the candidate FU Orionis star CB34FU (Yun et al. 1997; Alves et al. 1997). Two exceptions are FU Ori itself, with a peak flux density at 850 μm of only 0.078 Jy beam^{-1} at a distance of 450 pc, and BBW76, which is even fainter (0.013 Jy beam^{-1} at 1.3 mm). If CB34FU is similar to, but more distant than, FU Ori and BBW76, it would have a flux density < 0.010 Jy beam^{-1}, well below our detection limit. Thus, if CB34FU is indeed an FU Orionis star, then it would be another example of an FU Orionis star with a rather small accretion disk.

IRAS 19433+2743 in L 810

IRAS 19433+2743, detected at all four IRAS wavebands, is the only IRAS source within the optical core of L 810 (also known as CB 205), although one other IRAS source is detected at 60 μm or 100 μm in the envelope region as defined in the CB catalog. We have mapped only the field around IRAS 19433+2743, the colder of these two IRAS sources. We detect two submillimeter sources in our maps. L 810: SMM1 is a bright extended submillimeter source slightly northeast of the nominal IRAS source position (Fig. 3). We also find a fainter, spatially unresolved, submillimeter source (L 810: SMM2) located $38''$ west and $22''$ south of the L 810: SMM1. In the 850 μm map, we see that L 810: SMM1 and L 810: SMM2 lie at opposite ends of a shell-like structure which could contain additional embedded sources. This dust shell is also observed, though only marginally, in our lower signal-to-noise, 450 μm map.

The 450 μm and 850 μm emission from L 810: SMM1 is extended north-south, similar to the orientation of the bipolar reflection nebula observed in the optical (Scarrott et al. 1991; Neckel & Staude 1990) and near-infrared (Yun et al. 1993), and illuminated by the near-infrared source L 810 IRS. Previous studies of L 810 have revealed a large number of optical and near-infrared sources observed toward this globule. The positions of all the observed sources in the SCUBA field are overlayed on our submillimeter maps. All of these optical and near-infrared sources, with the exception of Star #6, have been suggested to be embedded within the globule (Neckel & Staude 1990; Neckel et al. 1985). Submillimeter peaks, possibly associated with Stars #7, #17, L 810IRS, and perhaps #8, can be seen within the extended emission from L 810: SMM1 at 450 μm, suggesting that these optical and near-infrared sources may be embedded within L 810. Thus,

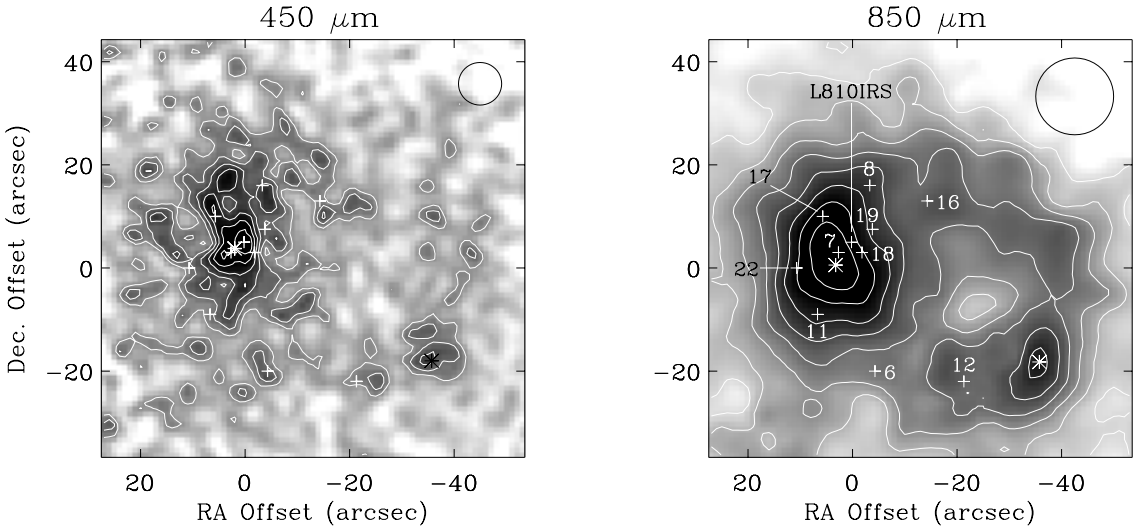

Fig. 3. 450 μm and 850 μm jiggle maps of the IRAS 19433+2743 field associated with L 810. The origin is located at the nominal IRAS source position. The position of L 810: SMM1 and L 810: SMM2 are identified by asterisks at (2″, 4″) and (−36″, −18″), respectively. The contours at 450 μm are drawn at 40, 50, 60, 70, 80, and 90% of the L 810: SMM1 peak (2.2 Jy beam^{-1}), while the contours at 850 μm are drawn at 20, 30, 40, 50, 60, 70, 80, and 90% of the L 810: SMM1 peak (0.47 Jy beam^{-1}). The 3-σ noise levels of the maps are 0.85 and 0.081 Jy beam^{-1} at 450 μm and 850 μm, respectively. The positions of optical and near-infrared sources located within this field are identified by plus signs. The sources are labeled using the notation of Neckel et al. (1985) and Neckel & Staude (1990).

L 810: SMM1 appears to coincide with the region containing the densest cluster of stars. No optical or near-infrared sources are seen in the direction of L 810 SMM2. SMM2 is therefore a likely Class 0 source.

One, or perhaps both of the submillimeter sources in L 810 is associated with a molecular outflow. The CO study by Yun & Clemens (1994a) shows an outflow centered very near L 810: SMM1, while the CO map by Xie & Goldsmith (1990) places the outflow center closer to L 810: SMM2. Each outflow study reveals a bipolar outflow oriented north-south with the peaks of red-shifted and blue-shifted emission separated by ∼45″ (one beam-width). The map of Xie & Goldsmith shows additionally an elongated lobe of redshifted emission protruding through the blue outflow lobe, suggesting that there could be more than one outflow in the region. However, until the outflows are observed with higher spatial resolution, it is impossible to securely identify which star or submillimeter source drives the outflow or whether there is more than one outflow in the region. L 810 IRS, the intermediate luminosity star (L_{bol} = 890 $L_\odot$), which Yun et al. (1993) identify as the source illuminating the reflection nebula, coincides with a strong peak in our 450 μm map, suggesting that it is associated with hot dust. However, at 850 μm the emission peaks more to the southwest indicating that there are other cooler embedded sources within the extended L 810: SMM1 core. Yun et al. also identify a near-infrared jet associated with #12 and note that it is aligned in the direction of L 810 IRS. However, our maps show that #12 is close to a dust peak, and therefore the jet could equally well be driven by, not terminate at, #12. Neckel et al. (1985) found an H_2O maser north of #12, suggesting this could be the source powering the outflow (Scappini et al. 1991). The presence of multiple outflow lobes, near-infrared jets, an H_2O maser, as well as a cavity surrounded by a shell of dust emission, strongly suggest that there are multiple outflow sources in L 810.

We derive a mass of ∼10 $M_\odot$ for L 810: SMM1 (Table 3), not including the surrounding cloud dust. Our result is consistent with the mass of 7.1 $M_\odot$ derived by Launhardt & Henning (1997) for the 1.3 mm counterpart and surrounding cloud within the 12″ beam used in their observations. The mass derived from our observations is understandably larger than that derived by Launhardt & Henning since they had assumed the source is unresolved for the purpose of estimating a mass. Our submillimeter maps demonstrate that L 810: SMM1 is one of the largest resolved sources in this study, and our derived mass is an estimate of the entire mass of this source. The large size of L 810: SMM1, as well as the difference in the 450 μm and 850 μm morphologies, indicate that the submillimeter source contains multiple sources. While L 810 IRS and some of the YSOs seen projected toward this core may be associated with some of the submillimeter emission, we suggest that the submillimeter emission originates from colder protostellar sources embedded in the cloud core (see Sect. 4).

We estimate that the cloud, including the mass associated with L 810: SMM1 and L 810: SMM2, contains ∼130 $M_\odot$ within our field (Tables 2 & 3), as much as a factor of two greater than that estimated from $C^{18}O$ and H_2CO observations (Wang et al. 1995), but in reasonable agreement with the mass estimate by Xie & Goldsmith (1990), who estimate 100–200 $M_\odot$ within 1′ of the center of the cloud.

L 810 thus appears to have star formation activity extending from optically visible PMS stars to the Class I illuminator, L 810IRS, to multiple, candidate Class 0 protostars. Much of the star formation activity is localized in the region surrounding L 810: SMM1. L 810 is a globule containing a large cluster of

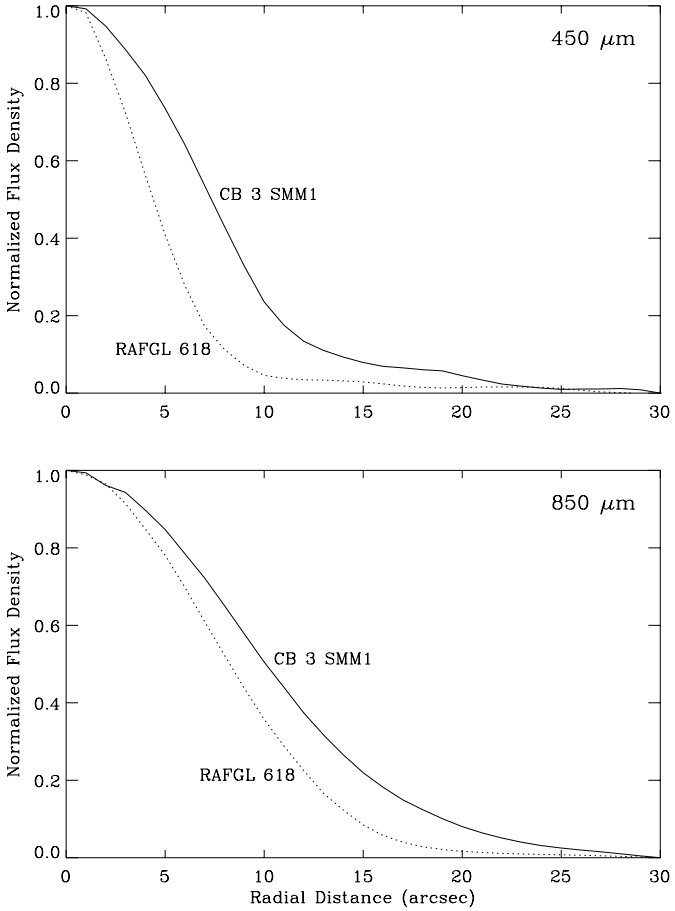

Fig. 4. Azimuthally averaged, radial flux density profiles of the compact sources CB 3: SMM1 and RAFGL 618 at 450 μm and 850 μm. RAFGL 618 is an unresolved or marginally resolved source, representing the 450 μm and 850 μm beam profiles. These profiles are normalized to the same peak flux density.

YSOs, with L 810: SMM2 being the youngest generation of star formation within this globule.

4. Discussion and conclusion

The three globules observed in this study are known to be associated with small clusters of low or intermediate mass YSOs, most of which are seen only in the near-infrared. CB 3 and L 810 have been mapped at K to a limiting magnitude of at least 18 (Launhardt et al. 1998b; Yun et al. 1993), while the near-infrared survey of CB 34 has a limiting magnitude of only $\sim$14.5 at K (Alves & Yun 1995). Given that a 1 $M_\odot$ PMS star (younger than 10 Myr) has an absolute magnitude of $\sim$2–3 (Baraffe et al. 1998), at least 4 magnitudes of circumstellar extinction at K are necessary to prevent PMS stars with masses greater than 1 $M_\odot$ from being detected at K for both CB 3 and L 810. In the case of CB 34, only 1 magnitude of K-band extinction would be sufficient to render a 1 $M_\odot$ PMS star undetectable in the K survey. Therefore, we expect that most Class I and Class II sources with masses $\geq$ 1 $M_\odot$ in these globules to have been detected in the near-infrared studies, with the possible exception of the youngest Class I sources in CB 34. By definition, Class 0 sources, if they exist in these large globules, will be below the detection limits in the completed near-infrared observations.

The IRAS sources in the three globules have 60 μm – 100 μm spectral colors indicative of cold protostellar sources and therefore represent the most probable sites for current star formation within these globules. These IRAS colors cannot be explained by the weakly embedded Class I and Class II sources previously observed in the near-infrared in the vicinity of the cold IRAS sources. Instead, the IRAS colors suggest that a population of very young, extremely embedded Class I sources or Class 0 protostars are present within these large globules. Our observations are consistent with this interpretation of the IRAS data, in that they have revealed submillimeter sources in the vicinity of the IRAS sources for all three large globules studied in this work.

The masses of almost all the submillimeter sources detected in our survey are comparable to the virial masses (Table 2), which suggests the sources are in virial equilibrium. However, we may have overestimated the virial masses in distant globules. The previously published, single dish observations from which we obtained linewidths are likely to be affected by gas along the line of sight through the cloud as well as from the dense core, whereas the dust emission originates from the core alone. Furthermore, a dark cloud forming a cluster likely is permeated by outflows from young stars and protostars, which may be sufficient to trigger collapse of cloud cores that otherwise would be gravitationally stable. This effect is seen very clearly in the active star forming region NGC 1333, where Knee & Sandell (2000) find about 10 outflows, some of which have excavated large cavities and triggered new star formation. The cavity in L 810 appears similar to the large cavity in NGC 1333 (Warin et al. 1996; Knee & Sandell 2000). In this respect, CB 34 also may be rather similar to L 810 and NGC 1333.

Evolved YSOs of Class I and Class II in nearby clouds are often detected as submillimeter sources with near-infrared counterparts. However, we suggest that if some of the submillimeter sources detected in our maps of large, distant globules are Class I or Class II sources rather than protostars, then they could only be intermediate-mass, Class I YSOs. This fact may be demonstrated by first considering HL Tau, one of the brightest low-mass, Class I sources at submillimeter wavelengths. If HL Tau were at a distance typical of these large globules (distance of $\sim$2 kpc), it would have an 850 μm flux density of only $\sim$15 mJy and thus would be undetectable in our submillimeter maps. On the other hand, a high-mass Class I source such as AFGL 490 (L_{bol} = 2.2 10^3 $L_\odot$; Chini et al. 1991) would easily be detected in our maps even at 2 kpc, where it would appear as an unresolved point source with an 850 μm flux of $\sim$1 Jy. However, the sources we have mapped have much lower luminosities than those typical of high-mass objects like GL 490. A better example of the type of Class I sources we may have detected in these large globules is NGC 2071 IRS (distance = 390 pc), having a luminosity of 590 $L_\odot$ (Butner et al. 1990). Note, however, that NGC 2071 IRS is actually three intermediate-mass YSOs within

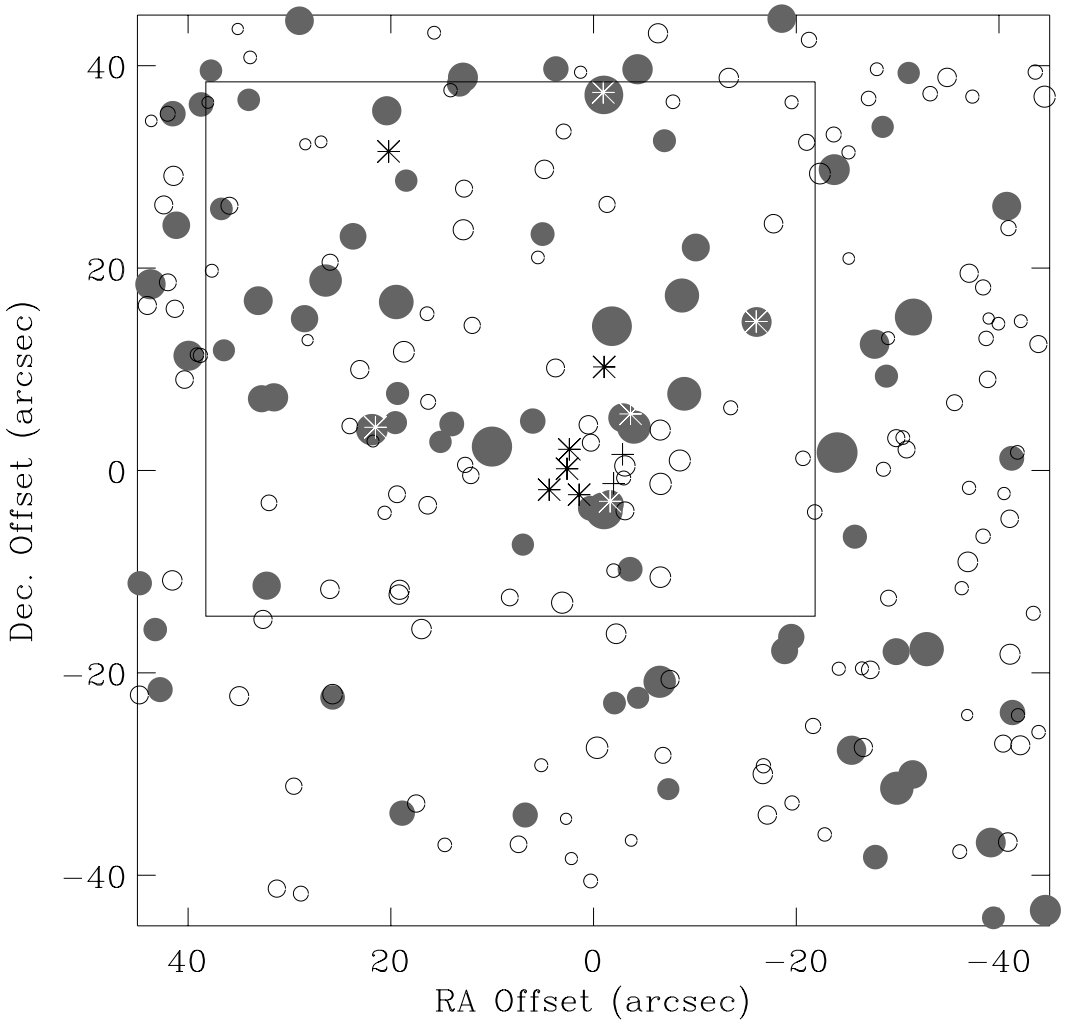

Fig. 5. K-band sources and submillimeter sources within the region toward the nearby star-forming core ρ Oph A, as it would appear if it were at a distance of 2 kpc and assuming all near-infrared sources toward this region are members of the cloud. Those K sources which would be detected by a near-infrared survey complete to K = 17 mag (comparable to the near-infrared surveys of CB 3 and L 810 which have limiting magnitudes of 18 at K) are identified by filled circles, while known sources which are too faint to be detected by such a survey are identified by open circles. In either case, the size of the circle is indicative of the brightness of the star (larger circles correspond to brighter stars). The positions and K magnitudes of these sources were taken from the catalog of Barsony et al. (1997). The figure shows that ∼80 of 220 sources would be detected by the K-band survey. However, the figure, representing all the near-infrared sources in this region, is contaminated by foreground sources which are not members of the ρ Oph A core. These foreground sources should not have been "moved" to 2 kpc. Assuming sources with J−H and H−K color excesses are YSOs and those without color excesses are not part of the ρ Oph A cluster, only a few dozen (rather than ∼80) sources remaining in the field would be detected in a near-infrared survey complete to K = 17 mag, consistent with near-infrared surveys of regions of comparable size within the large globules. Because the K sources within ∼10″ of the center of the field have near-infrared excesses, the conclusion within the text concerning source confusion among near-infrared and submillimeter sources are unaffected by the presence of foreground sources within the figure. The rectangle represents that portion of the field for which submillimeter observations are available in the literature (Wilson et al. 1999; André et al. 1993). The submillimeter sources are identified by asterisks and plus signs. The black asterisks identify the positions of prestellar, preprotostellar, and protostellar sources found within the region, while the white asterisks overlaying a few stars identify the Class I or Class II sources detected in the submillimeter. The plus signs identify the positions of submillimeter continuum sources associated with bow shocks from the VLA 1623 outflow. Note that the well-studied protostar VLA 1623 and prestellar clumps SM 1, SM 1N, and SM 2 are identified by the four asterisks clustered near the origin. The $1\farcm5 \times 1\farcm5$ field, centered on RA = $16^h\ 26^m\ 25^s$ Dec = $-24^\circ\ 24'$ (2000.0), is comparable in size to the fields of our SCUBA maps.

a 10″ region (Walther et al. 1991; Bally & Predmore 1983; Persson et al. 1981) which, at 2 kpc, would appear unresolved at 850 μm with a flux of ∼600 mJy (Sandell 1994).

Although some of the submillimeter sources detected in our submillimeter maps may be intermediate-mass, Class I YSOs, we suggest that most are likely to be Class 0 protostars. Let us consider submillimeter maps of nearby, star-

forming, molecular clouds having similar masses and luminosities as the large globules observed here. For example, the star-forming cluster NGC 1333 (distance = 220 pc; Cernis 1990) contains more than a hundred low-mass, reddened near-infrared sources (Lada et al. 1996; Aspin et al. 1994), but we would see only ∼20 of these YSOs if NGC 1333 were at a distance of 2 kpc. In addition to the near-infrared population of young stars, NGC 1333 contains a population of protostars, observable only in the submillimeter and far-infrared. Sandell & Knee (2000) find about 30 submillimeter sources in the central $13' \times 18'$ area of NGC 1333. The majority of these submillimeter sources are known Class 0 sources such as IRAS 4, while a smaller fraction likely are prestellar cores. Only two submillimeter sources can be readily identified with Class I YSOs. Therefore, we conclude that most, if not all, of the submillimeter sources in our maps of the distant, large globules are young, Class 0 protostars rather than Class I sources.

To strengthen our interpretation that the submillimeter sources are protostars, we now look at how the ρ Ophiuchi molecular cloud (distance = 160 pc) would appear in the near-infrared and submillimeter, if it was at a distance of 2 kpc. Fig. 5 illustrates the region approximately centered on the star-forming core ρ Oph A, containing the protostar VLA 1623 and the prestellar clumps SM 1, SM 1N, and SM 2 (André et al. 1993). Within the portion of the field for which submillimeter observations have been published, the population of submillimeter sources includes five evolved YSOs (Class I and Class II sources), one protostar, five prestellar or preprotostellar clumps, and two submillimeter sources associated with bow shocks. Given the sensitivity of our submillimeter maps, if the ρ Oph molecular cloud were at a distance of 2 kpc, only one submillimeter source – representing the blended emission from VLA 1623, SM 1, SM 1N, and SM 2 – would be detectable (the integrated 850 μm emission would be ∼150 mJy). Because this submillimeter source would be extended and would be found within a few arcseconds of several sources detectable at K, the submillimeter source would appear to have at least one near-infrared counterpart. However, our existing knowledge of ρ Oph demonstrates that identifying the submillimeter source with any of the apparent near-infrared counterparts would be erroneous and would lead us to misclassify the submillimeter source as an evolved YSO.

The submillimeter sources detected in our maps have rather large sizes 0.07–0.2 pc and have masses from 1–40 $M_\odot$ (Table 2), at least an order of magnitude greater than those of low-mass protostars found in Bok globules (Huard et al. 1999). The large sizes and masses suggest that the submillimeter sources detected in our observations may each consist of more than one protostar. That this would be the case is well illustrated by ρ Oph, but it is even more striking in NGC 1333. For example, IRAS 4, the brightest submillimeter source in NGC 1333, is a small cluster of two binary protostars and a fainter single protostar, all within a $30''$ radius (Lay et al. 1995; Sandell et al. 1991). At 2 kpc, the entire IRAS 4 complex would be unresolved and almost blend into IRAS 3, also known as the SSV 13 ridge (Chini et al. 1997a), containing another three submillimeter sources. Of all the sources in IRAS 3 and IRAS 4, only one (SSV 13) is a Class I object. Therefore, we expect that the submillimeter emission from the sources detected in our maps is primarily from small clusters of Class 0 protostars perhaps blended with one or more Class I sources.

Throughout our discussion, we have made use of our existing knowledge of the YSO populations of nearby star-forming regions in order to interpret our submillimeter maps of the distant, large globules. We expect that the population distributions of YSOs (i.e., the relative numbers of protostars compared with Class I and Class II sources) within large globules to be similar to that within the nearby star-forming regions since the large globules are comparable in actual size and mass to the nearby molecular clouds. We have derived masses of at least ∼100 $M_\odot$ for the gas and dust associated with the large globules and their embedded submillimeter sources. The masses of these large globules are certainly greater than 100 $M_\odot$ since our observations are only sensitive to the densest regions of the globules. Furthermore, we have mapped only fractions of entire globules. The optical extent of the large globules are typically 1–5 pc across (Clemens & Barvainis 1988). For comparison, the molecular clouds in the nearby, star-forming region of Taurus-Auriga are typically 3–10 pc across and have masses 10^2–10^3 $M_\odot$ (Ungerechts & Thaddeus 1987).

We have argued that most submillimeter sources mapped in our observations are small clusters of young, embedded protostars. Thus, the three large globules – CB 3, CB 34, and L 810 – are currently adding members to the YSO clusters. This finding suggests that cluster formation in large globules is a process that occurs over millions of years, consistent with previous studies of cluster formation in nearby large molecular clouds such as Orion, ρ Ophiuchus, and Serpens (e.g., Palla & Stahler 1999; Johnstone & Bally 1999; Wilson et al. 1999; Testi & Sargent 1998; Chini et al. 1997b; Hillenbrand 1997; Hurt & Barsony 1996; Casali et al. 1993).

Acknowledgements. The work of Huard and Weintraub is supported by a NASA grant NAG54428.

References

Alves J.F., Yun J.L., 1995, ApJ 438, L107
Alves J., Hartmann L., Brice C., Lada C.J., 1997, AJ 113, 1395
André P., Ward-Thompson D., Barsony M., 1993, ApJ 406, 122
Aspin C., Sandell G., Russell A.P.G., 1994, A&AS 106, 165
Bally J., Predmore R., 1983, ApJ 265, 778
Baraffe I., Chabrier G., Allard F., Hauschildt P.H., 1998, A&A 337, 403
Barsony M., Kenyon S.J., Lada E.A., Teuben P.J., 1997, ApJS 112, 109
Bourke T.L., Hyland A.R., Robinson G., James S.D., Wright C.M., 1995, MNRAS 276, 1067
Butner H.M., Evans N.J., Mundy L.G., Natta A., Ranich M.S., 1990, ApJ 364, 164
Casali M.M., Eiroa C., Duncan W.D., 1993, A&A 275, 195
Cernis, K., 1990, Ap&SS 166, 315
Chandler C.J., Sargent A., 1993, ApJ 414, L29
Chini R., Henning Th., Pfau W., 1991, A&A 247, 157
Chini R., Reipurth B., Sievers A., et al., 1997a, A&A 325, 542

Chini R., Reipurth B., Ward-Thompson D., et al., 1997b, ApJ 474, L135
Clemens D.P., Barvainis R., 1988, ApJS 68, 257
Codella C., Bachiller R., 1999, A&A 350, 659
Codella C., Scappini F., 1998, MNRAS 298, 1092
Gear W.K., Cunningham C.R., 1995, in: Emerson D.T., Payne J.M. (eds.), ASP Conf. Ser. 75,darin: Multifeed Systems for Radio Telescopes, San Francisco: ASP, p. 215
Hildebrand R.H., 1983, QJRAS 24, 267
Hillenbrand L.A., 1997, AJ 113, 1733
Huard T.L., Sandell G., Weintraub D.A., 1999, ApJ 526, 833
Hurt R.L., Barsony M., 1996, ApJ 460, L45
Jijina J., Myers P.C., Adams F.C., 1999, ApJS 125, 161
Johnstone D., Bally J., 1999, ApJ 510, L49
Knee L.B.G, Sandell G., 2000, A&A, submitted
Lada C.J., Alves J., Lada E.A., 1996, AJ 111, 1964
Launhardt R., Henning T., 1997, A&A 326, 329
Launhardt R., Evans II N.J., Wang Y., et al., 1998a, ApJS 119, 59
Launhardt R., Henning T., Klein R., 1998b, in: Yun J.L., Liseau R. (eds.), ASP Conf. Ser. 132, Star Formation with the Infrared Space Observatory, San Francisco: ASP, p. 119
Launhardt R., Ward-Thompson D., Henning Th., 1997, MNRAS 288, L45
Lay O.P., Carlstrom J.E., Hills R.E., 1995, ApJ 452, L73
MacLaren I., Richardson K.M., Wolfendale A.M., 1988, ApJ 333, 821
Motte F., André P., Neri R., 1998, A&A 336, 150
Neckel T., Staude H.J., 1990, A&A 231, 165
Neckel T., Chini R., Güsten R., Wink J.E., 1985, A&A 153, 253
Palla F., Stahler S.W., 1999, ApJ 525, 772
Persson S.E., Geballe T.R., Simon T., Lonsdale C.J., Baas F., 1981, ApJ 251, L85
Sandell, G., 1994, MNRAS 271, 75
Sandell G., 1997, "SCUBA mapping cookbook: A first step to proper map reduction," Starlink Document sc11
Sandell G., Knee L.B.G, 2000, in: Wootten A. (ed.), ASP Conf. Ser., Science with the Atacama Large Millimeter Array, San Francisco: ASP,
Sandell G., Aspin C., Duncan W.D., Russell A.P.G., Robson E.I., 1991, ApJ 376, L17
Scappini F., Caselli P., Palumbo G.G.C., 1991, MNRAS 249, 763
Scarrott S.M., Rolph C.D., Tadhunter C.N., 1991, MNRAS 248, 27
Testi L., Sargent A.I., 1998, ApJ 508, L91
Ungerechts H., Thaddeus P., 1987, ApJS 63, 645
Visser A.E., Richer J.S., Chandler C.J., Padman R., 1998, MNRAS 301, 585
Walther D.M., Geballe T.R., Robson E.I., 1991, ApJ 377, 246
Wang Y., Evans II N.J., Zhou S., Clemens D.P., 1995, ApJ 454, 217
Warin S., Casterts A., Langer W.D., Wilson R.W., Pagani L., 1996, A&A 306, 935
Weintraub D.A., Sandell G., 1991, ApJ 382, 270
Wilson C.D., Avery L.W., Fich M., et al., 1999, ApJ 513, 139
Wright M., Sandell G., Wilner D.J., Plambeck R.L., 1992, ApJ 393, 225
Xie T., Goldsmith P.F., 1990, ApJ 359, 378
Yun J.L., Clemens D.P., 1990, ApJ 365, L73
Yun J.L., Clemens D.P., 1992, ApJ 385, L21
Yun J.L., Clemens D.P., 1994a, ApJS 92, 145
Yun J.L., Clemens D.P., 1994b, AJ 108, 612
Yun J.L., Clemens D.P., 1995, AJ 109, 742
Yun J.L., Clemens D.P., McCaughrean M.J., Rieke M., 1993, ApJ 408, L101
Yun J.L., Moreira M.C., Alves J.F., Storm J., 1997, A&A 320, 167